Assessment of boundary-element method for modelling a free-floating sloped wave energy device. Part 1: numerical modelling.

Grégory S. Payne [*] , Jamie R.M. Taylor, Tom Bruce,

Penny Parkin

Institute for Energy Systems, School of Engineering and Electronics, University of Edinburgh, Edinburgh EH9 3JL, UK

Abstract

Boundary element method has been widely used as a design tool in the offshore and ship building industry for more than 30 years. Its application to wave energy conversion is however more recent. This paper deals with the numerical modelling of a free-floating sloped wave energy device. The power take-off mechanism of the device consists of an immersed tube with a piston sliding inside. The modelling is done using the boundary-element method package WAMIT. The model is first worked out for the case where the axis of the tube is vertical. It is then derived for the tube inclined and successfully verified against numerical benchmark data. A companion paper presents results of a detailed comparison with a physical model study.

Key words: wave energy, numerical modelling, boundary element method, WAMIT

1 Introduction

Computer-based numerical prediction of wave-body interactions has become a powerful design tool and is widely used in the offshore industry. The most commonly used approach for investigating the behaviour of large structures in waves is the boundary-element method based on Green functions. The underlying theory for this technique was developed in the 1960s. It was not however until the 70s that the availability of relatively powerful computers made these numerical models practically attractive, although these mainframe machines were available only in a few institutions. In recent years, the improvement of computer technology and numerical algorithms makes it possible to study complex body shapes on desktop computers.

Boundary-element methods are based on potential flow theory which is associated with four key assumptions: incompressibility and constant density of the fluid, zero viscosity and irrotationality. Furthermore in the boundary-element method discussed in this paper, body surface and free surface boundary conditions are linearised. That implies that the oscillation amplitudes of both the fluid and the body are small relative to the cross-sectional dimensions of the body and the wavelength. All these assumptions bring limitations and from a generic point of view, the scope of these limitations is difficult to assess precisely. A large body of experience from the offshore industry provides some guidelines on the validity of such methods (Herfjord and Nielsen, 1992; Eatock Taylor and Jefferys, 1986). The application to wave energy conversion is however more recent (Lee et al., 1996; Delauré and Lewis, 2003) and the

* Corresponding author.
  Email address: `gregory.payne@ed.ac.uk` (Grégory S. Payne).

wide variety of devices and body shapes encountered in this field render the knowledge of these limitations much less comprehensive.

The present work investigates the numerical modelling of a free-floating, sloped wave energy device using the boundary-element method package WAMIT (WAMIT, Inc., 2000). The wave energy converter concept considered consists of a buoy head and of a power take-off mechanism. The latter is inspired by that of the device developed by the Swedish company Inter Project Services AB (Bergdahl, 1992). This mechanism can be operated with no reference to the seabed and therefore allows operation in deep water. It carries its own internal reaction mass in the form of a body of water contained in a large inclined pipe which is open to the sea at both ends. Waves force the buoy to move but the large water mass tends to stay relatively fixed in space so that work can be done between a piston in the pipe and an oil hydraulic ram attached to the buoy head. Figure 1 shows a schematic of the system.

The sloped feature was originally introduced by Stephen Salter (Salter and Lin, 1995) and intends to make the device more efficient in longer waves.

The predominant motions of free-floating wave energy converters are cyclic and their response therefore depends on the frequency of the exciting waves. At wave period corresponding to the natural frequency of the device, motions are generally more pronounced. If these are suitably harvested, maximum power is generated. Given that long waves contain more energy than short ones of the same amplitude, there is a case for designing wave energy converters with long natural periods. As a first approximation, natural period T_0 can be considered as proportional to the square root of the inertia M of the device divided by
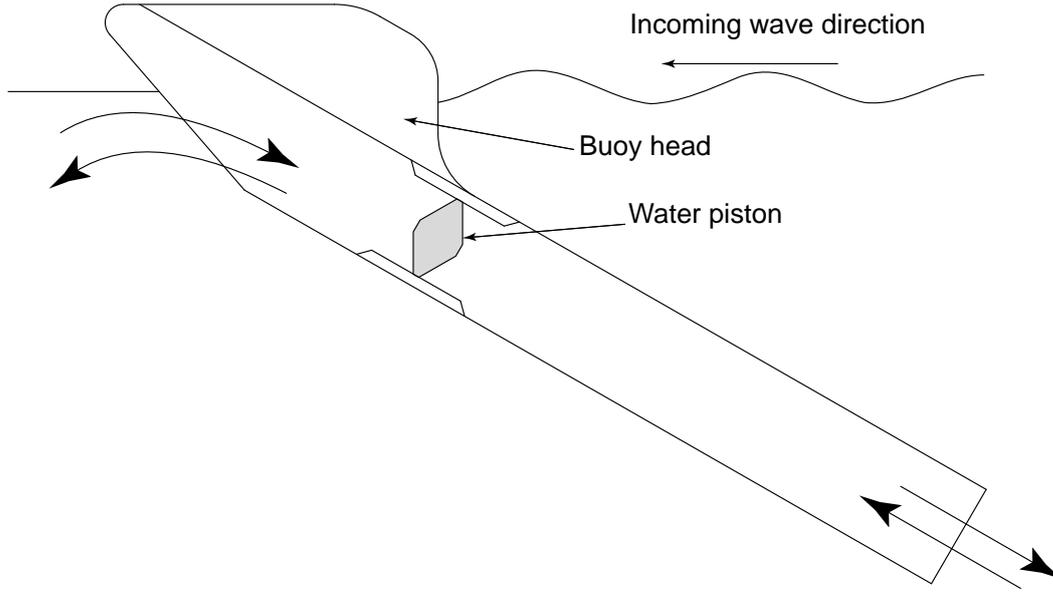
Fig. 1. Cross section of the sloped wave energy converter concept. The large arrows indicate where the water is able to flow in and out of the power take-off tube.

its hydrostatic stiffness S.

$$T_0 \propto \sqrt{\frac{M}{S}} \tag{1}$$

Longer natural period can therefore be achieved by increasing the mass (or the added mass) of the device or by reducing the hydrostatic stiffness.

The former approach can lead to bigger and heavier devices with increased structural costs. The hydrostatic stiffness associated with buoyancy is directed vertically. Thus by restraining the motion of a device to an intermediate direction between surge and heave, the component of stiffness that acts in the principal direction of motion is reduced.

The WAMIT modelling of the power take-off mechanism with the piston sliding inside the tube requires special attention. It is first worked out in the case

where the axis of the power take-off tube is vertical. The modelling of the sloped configuration is subsequently derived and verified against numerical benchmark data.

Detailed comparison with physical model data is presented in the companion paper.

2 Modelling considerations

The power take-off mechanism basically consists of two components:

- A circular tube, rigidly connected to the buoy. This tube is fully submerged and both its ends are open. It is thus flooded.
- A piston, whose diameter corresponds to the inner diameter of the tube. The piston is located inside the tube and can slide back and forth along the axis of the tube. The seal between the piston and the tube is as leak tight as is practical, thus preventing water from flowing freely from one side of the tube to the other.

The main difficulty in modelling such a power take-off mechanism with WAMIT lies in the relative motion between the piston and the tube. The device consists of two rigid bodies (the piston and the rest of the device) whose motions relative to each other have to be accurately constrained.

In order to work out and to verify a formulation that reasonably models the power take-off, a simple geometry was used within WAMIT. This geometry consists of a piston, a tube and a float, but they do not have the complexity of the actual experimental model and they are designed in a way that minimises
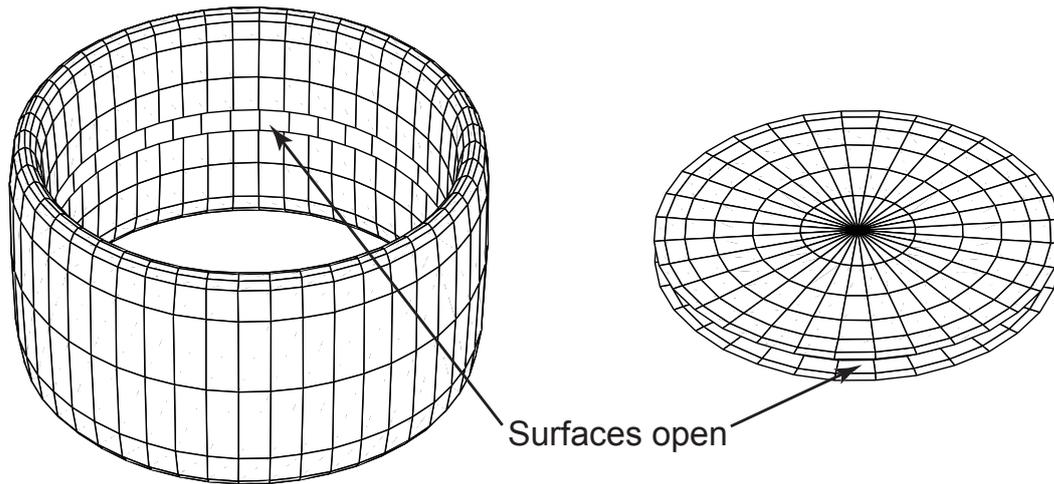
Fig. 2. 'Open surfaces' representation of the tube (left) and the piston (right).
convergence issues.

3 General modelling formulation

Focusing on the piston and the tube, both bodies are defined as shown on figure 2 with 'open surfaces'. When these two bodies are combined the resulting geometry represents realistically the tube with the piston inside, at rest. The fact that WAMIT is based on linear hydrodynamic theory implies that the fluid velocity potential and the hydrodynamic pressure are derived from geometries corresponding to bodies at rest (see chapter six of (Newman, 1977)). Thus, in the geometry definition, there is no need to account for actual movements of the piston.

Two aspects of the formulation are of particular importance:

- WAMIT computes the hydrostatic data by expressing them in the form of surface integrals over the wetted surface of the body. This approach is

based on Gauss' divergence theorem (WAMIT, Inc., 2000; Payne, 2006). Since each body taken individually does not represent a closed surface (see figure 2), WAMIT computes incorrect hydrostatic restoring coefficients.

- The equation of motion of the two-body system needs to include terms that restrain the motion of the piston relative to the tube so that the piston only moves in translation along the tube axis.

3.1 Hydrostatic corrective terms

As mentioned above, when dealing with geometries defined by open surfaces, WAMIT derives erroneous hydrostatic quantities. The hydrostatic matrix cannot be directly modified by the user. The equation of motion solved by WAMIT is given by:

$$-\omega^2(\mathbf{M}^E + \mathbf{A})\boldsymbol{\xi} + i\omega(\mathbf{B} + \mathbf{B}^E)\boldsymbol{\xi} + (\mathbf{C} + \mathbf{C}^E)\boldsymbol{\xi} = \mathbf{F}_{exc} \qquad (2)$$

where ω is the radian frequency, $\boldsymbol{\xi}$ the response amplitude operator vector, $\mathbf{M}^E$ is the inertia matrix of the body, $\mathbf{A}$ is the added mass matrix, $\mathbf{B}$ is the radiation damping matrix, $\mathbf{C}$ is the hydrostatic stiffness matrix, $\mathbf{C}^E$ is the external stiffness matrix and $\mathbf{F}_{exc}$ is the wave exciting force vector. More details on equation (2) can be found in (Lee, 1995).

It can be seen from equation (2) that incorrect terms in $\mathbf{C}$ can be accounted for by introducing corrective terms in $\mathbf{C}^E$, which is entirely defined by the user.

The appropriate corrective terms are derived by the following procedure:

- WAMIT is run for the open surface geometries in order to get the erroneous

hydrostatic matrices.

- WAMIT is used to calculate the hydrostatic matrix of each body taken individually. For this purpose, the geometry of each body is 'closed' thus avoiding the problems related to open surfaces.

- The erroneous 'open body' matrices are subtracted from the 'closed body' matrices to yield the 'hydrostatic corrective' matrix.

3.2   Constraint of the piston motion

For the power take-off to be modelled realistically, it must be ensured that the piston motion is restrained to translation along the tube axis only and that this movement of translation relative to the tube can be damped.

Constraint of the piston motion can be achieved by applying high stiffness between the tube and the piston. This is done through the external stiffness matrix $\mathbf{C}^E$. Damping the piston motion is implemented through the external damping matrix $\mathbf{B}^E$.

The $\mathbf{C}^E$ and $\mathbf{B}^E$ matrices are first derived for the simpler case where the tube is vertical. They are then obtained for the inclined tube using transformation matrices. For both cases, the geometry of the bodies exhibit a vertical plane of symmetry where the wave direction of propagation lies. This allows the number of degrees of freedom to be investigated to be reduced to three per body - surge, heave and pitch.

4 Vertical axis formulation

The power take-off tube is here considered to be vertical. When devising the coefficients of the external stiffness matrix, it is important to note that since the system, as a whole, is free floating, no component of the stiffness force vector should be a function of the displacement components of only one body. If this was the case, it would mean that one of the bodies would be restrained with respect to the global frame of reference. In other words, the external stiffness should only restrain the motion of the first body with respect to the second.

The stiffness relation is given by the following equation:

$$\mathbf{F} = \mathbf{C}^E \boldsymbol{\xi} \tag{3}$$

where $\mathbf{F}$ is the resulting stiffness force vector.

The requirements on the six components of interest of $\mathbf{F}$, for restraining the motion of the piston along the tube axis are the following:

$$f_1 = (\xi_1 - \xi_7)s_t \tag{4}$$
$$f_3 = 0 \tag{5}$$
$$f_5 = (\xi_5 - \xi_{11})s_r \tag{6}$$
$$f_7 = (\xi_7 - \xi_1)s_t \tag{7}$$
$$f_9 = 0 \tag{8}$$
$$f_{11} = (\xi_{11} - \xi_5)s_r \tag{9}$$

where f_j and ξ_j are the components of vectors $\mathbf{F}$ and $\boldsymbol{\xi}$ respectively. The indices $j = 1 \ldots 6$ correspond to first body surge, sway, heave, roll, pitch and yaw respectively. The indices $j = 7 \ldots 12$ correspond to the modes of motion of the second body with the same convention as for the first. s_t and s_r are

9

very high stiffness values in translation and rotation respectively. This leads to the following stiffness matrix:

$$
\mathbf{C}^E =
\begin{pmatrix}
s_t & 0 & 0 & 0 & 0 & 0 & -s_t & 0 & 0 & 0 & 0 & 0 \\
0 & 0 & 0 & 0 & 0 & 0 & 0 & 0 & 0 & 0 & 0 & 0 \\
0 & 0 & 0 & 0 & 0 & 0 & 0 & 0 & 0 & 0 & 0 & 0 \\
0 & 0 & 0 & 0 & 0 & 0 & 0 & 0 & 0 & 0 & 0 & 0 \\
0 & 0 & 0 & 0 & s_r & 0 & 0 & 0 & 0 & 0 & -s_r & 0 \\
0 & 0 & 0 & 0 & 0 & 0 & 0 & 0 & 0 & 0 & 0 & 0 \\
-s_t & 0 & 0 & 0 & 0 & 0 & s_t & 0 & 0 & 0 & 0 & 0 \\
0 & 0 & 0 & 0 & 0 & 0 & 0 & 0 & 0 & 0 & 0 & 0 \\
0 & 0 & 0 & 0 & 0 & 0 & 0 & 0 & 0 & 0 & 0 & 0 \\
0 & 0 & 0 & 0 & 0 & 0 & 0 & 0 & 0 & 0 & 0 & 0 \\
0 & 0 & 0 & 0 & -s_r & 0 & 0 & 0 & 0 & 0 & s_r & 0 \\
0 & 0 & 0 & 0 & 0 & 0 & 0 & 0 & 0 & 0 & 0 & 0
\end{pmatrix}
\tag{10}
$$

Similarly, in order to damp the piston's vertical motion relative to the tube, the external damping matrix must be derived according to the following equations:

$$
f_3 = (\xi_3 - \xi_9)b \tag{11}
$$
$$
f_9 = (\xi_9 - \xi_3)b \tag{12}
$$

where b is the damping coefficient. This yields the external damping matrix

(13):

$$\mathbf{B}^E = \begin{pmatrix} 0 & 0 & 0 & 0 & 0 & 0 & 0 & 0 & 0 & 0 & 0 & 0 \\ 0 & 0 & 0 & 0 & 0 & 0 & 0 & 0 & 0 & 0 & 0 & 0 \\ 0 & 0 & b & 0 & 0 & 0 & 0 & 0 & -b & 0 & 0 & 0 \\ 0 & 0 & 0 & 0 & 0 & 0 & 0 & 0 & 0 & 0 & 0 & 0 \\ 0 & 0 & 0 & 0 & 0 & 0 & 0 & 0 & 0 & 0 & 0 & 0 \\ 0 & 0 & 0 & 0 & 0 & 0 & 0 & 0 & 0 & 0 & 0 & 0 \\ 0 & 0 & 0 & 0 & 0 & 0 & 0 & 0 & 0 & 0 & 0 & 0 \\ 0 & 0 & 0 & 0 & 0 & 0 & 0 & 0 & 0 & 0 & 0 & 0 \\ 0 & 0 & -b & 0 & 0 & 0 & 0 & 0 & b & 0 & 0 & 0 \\ 0 & 0 & 0 & 0 & 0 & 0 & 0 & 0 & 0 & 0 & 0 & 0 \\ 0 & 0 & 0 & 0 & 0 & 0 & 0 & 0 & 0 & 0 & 0 & 0 \\ 0 & 0 & 0 & 0 & 0 & 0 & 0 & 0 & 0 & 0 & 0 & 0 \end{pmatrix} \tag{13}$$

5   Inclined axis formulation

The principles are the same as for the vertical case, but the formulation is more complicated as the axis of motion of the piston does not correspond directly to one of the degrees of freedom.

Consider the body fixed coordinate system $\boldsymbol{L} : (O_L, \mathbf{i}_L, \mathbf{j}_L, \mathbf{k}_L)$ with respect to

11

which the geometry is defined. WAMIT requires that $\mathbf{k}_L$ is orientated vertically and pointing upwards. Now consider another body fixed coordinate system $\boldsymbol{I} : (O_I, \mathbf{i}_I, \mathbf{j}_I, \mathbf{k}_I)$ whose origin is the same as for $\boldsymbol{L}$ ($O_I = O_L$) and with $\mathbf{j}_I = \mathbf{j}_L$ but with $\mathbf{k}_I$ parallel to the axis of the tube and pointing upwards (see figure 3).
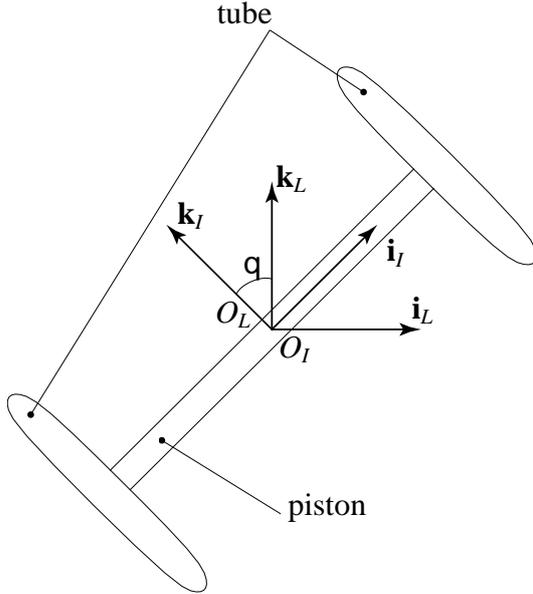

Fig. 3. Section view of the power take-off tube with piston showing the coordinate systems $\boldsymbol{L}$ and $\boldsymbol{I}$.

The formulation that has been derived to constrain and to damp the piston motion for the vertical case can be directly applied to the inclined case but using the inclined coordinate system $\boldsymbol{I}$. The external stiffness and damping matrices ($\mathbf{C}^E$ and $\mathbf{B}^E$ respectively) have however to be defined in the coordinate system $\boldsymbol{L}$. It is thus necessary to derive a transformation matrix that enables $\mathbf{C}^E$ and $\mathbf{B}^E$ to be described in $\boldsymbol{L}$ (denoted as $\mathbf{C}_L^E$ and $\mathbf{B}_L^E$) from $\mathbf{C}^E$

and $\mathbf{B}^E$ described in $\boldsymbol{I}$ (denoted as $\mathbf{C}_I^E$ and $\mathbf{B}_I^E$).

A general treatment of transformation matrices can be found in (Mortenson, 1997). $\mathbf{C}^E$ and $\mathbf{B}^E$ are 12×12 matrices. In three-dimensional space, transformation matrices are only 3×3. The fact that these matrices have 12×12 coefficients does however not imply that they express a linear transformation in twelve-dimension space. Instead, they relate to vectors that can be decomposed along three non-collinear unit vectors. As an example, the decomposition of the response amplitude operator vector $\boldsymbol{\xi}$, in the case of a two-body

approach yields:

$$
\boldsymbol{\xi} =
\begin{pmatrix}
\xi_1 \\
\xi_2 \\
\xi_3 \\
\xi_4 \\
\xi_5 \\
\xi_6 \\
\xi_7 \\
\xi_8 \\
\xi_9 \\
\xi_{10} \\
\xi_{11} \\
\xi_{12}
\end{pmatrix}
= \xi_1\mathbf{i} + \xi_2\mathbf{j} + \xi_3\mathbf{k} + \xi_4\mathbf{i} + \xi_5\mathbf{j} + \xi_6\mathbf{k} + \xi_7\mathbf{i} + \xi_8\mathbf{j} + \xi_9\mathbf{k} + \xi_{10}\mathbf{i} + \xi_{11}\mathbf{j} + \xi_{12}\mathbf{k} \tag{14}
$$

The 12×12 transformation matrix can thus be built by blocks; that is, repeating four times diagonally the standard 3×3 transformation matrix.

Let θ be the inclination angle between the $\boldsymbol{I}$ and $\boldsymbol{L}$ vertical axes: $\widehat{\mathbf{k}_I, \mathbf{k}_L} = \theta$. Those two coordinate systems share a common axis $(\mathbf{j}_I = \mathbf{j}_L)$. The 3×3

transformation matrix from $\boldsymbol{I}$ to $\boldsymbol{L}$ is thus:

$$
\mathbf{T}_{\substack{L/I \\ 3\times3}} = \begin{pmatrix} \mathbf{i}_L \cdot \mathbf{i}_I & \mathbf{i}_L \cdot \mathbf{j}_I & \mathbf{i}_L \cdot \mathbf{k}_I \\ \\ \mathbf{j}_L \cdot \mathbf{i}_I & \mathbf{j}_L \cdot \mathbf{j}_I & \mathbf{j}_L \cdot \mathbf{k}_I \\ \\ \mathbf{k}_L \cdot \mathbf{i}_I & \mathbf{k}_L \cdot \mathbf{j}_I & \mathbf{k}_L \cdot \mathbf{k}_I \end{pmatrix} = \begin{pmatrix} \cos\theta & 0 & -\sin\theta \\ \\ 0 & 1 & 0 \\ \\ \sin\theta & 0 & \cos\theta \end{pmatrix} \tag{15}
$$

And the 12×12 transformation matrix is:

$$
\mathbf{T}_{\substack{L/I \\ 12\times12}} = \begin{pmatrix} \mathbf{T}_{\substack{L/I \\ 3\times3}} & 0 & \cdots & 0 \\ \\ 0 & \mathbf{T}_{\substack{L/I \\ 3\times3}} & \ddots & \vdots \\ \\ \vdots & \ddots & \mathbf{T}_{\substack{L/I \\ 3\times3}} & 0 \\ \\ 0 & \cdots & 0 & \mathbf{T}_{\substack{L/I \\ 3\times3}} \end{pmatrix} \tag{16}
$$

$\mathbf{C}_L^E$ can be derived from $\mathbf{C}_I^E$ as follow:

$$
\mathbf{C}_L^E = \mathbf{T}_{L/I} \cdot \mathbf{C}_I^E \cdot \mathbf{T}_{L/I}^T \tag{17}
$$

and

$$
\mathbf{B}_L^E = \mathbf{T}_{L/I} \cdot \mathbf{B}_I^E \cdot \mathbf{T}_{L/I}^T \tag{18}
$$

where $\mathbf{T}_{L/I}^T$ is the transpose of $\mathbf{T}_{L/I}$.

This yields:

$$
\mathbf{C}_L^E =
$$

$$
\begin{pmatrix}
s_t\cos^2\theta & 0 & s_t\cos\theta\sin\theta & 0 & 0 & 0 & -s_t\cos^2\theta & 0 & -s_t\cos\theta\sin\theta & 0 & 0 & 0 \\
0 & 0 & 0 & 0 & 0 & 0 & 0 & 0 & 0 & 0 & 0 & 0 \\
s_t\cos\theta\sin\theta & 0 & s_t\sin^2\theta & 0 & 0 & 0 & -s_t\cos\theta\sin\theta & 0 & -s_t\sin^2\theta & 0 & 0 & 0 \\
0 & 0 & 0 & 0 & 0 & 0 & 0 & 0 & 0 & 0 & 0 & 0 \\
0 & 0 & 0 & 0 & s_r & 0 & 0 & 0 & 0 & 0 & -s_r & 0 \\
0 & 0 & 0 & 0 & 0 & 0 & 0 & 0 & 0 & 0 & 0 & 0 \\
-s_t\cos^2\theta & 0 & -s_t\cos\theta\sin\theta & 0 & 0 & 0 & s_t\cos^2\theta & 0 & s_t\cos\theta\sin\theta & 0 & 0 & 0 \\
0 & 0 & 0 & 0 & 0 & 0 & 0 & 0 & 0 & 0 & 0 & 0 \\
-s_t\cos\theta\sin\theta & 0 & -s_t\sin^2\theta & 0 & 0 & 0 & s_t\cos\theta\sin\theta & 0 & s_t\sin^2\theta & 0 & 0 & 0 \\
0 & 0 & 0 & 0 & 0 & 0 & 0 & 0 & 0 & 0 & 0 & 0 \\
0 & 0 & 0 & 0 & -s_r & 0 & 0 & 0 & 0 & 0 & s_r & 0 \\
0 & 0 & 0 & 0 & 0 & 0 & 0 & 0 & 0 & 0 & 0 & 0
\end{pmatrix}
\tag{19}
$$

and

$$\mathbf{B}_L^E =$$

$$
\begin{pmatrix}
b\sin^2\theta & 0 & -b\cos\theta\sin\theta & 0 & 0 & 0 & -b\sin^2\theta & 0 & b\cos\theta\sin\theta & 0 & 0 & 0 \\
0 & 0 & 0 & 0 & 0 & 0 & 0 & 0 & 0 & 0 & 0 & 0 \\
-b\cos\theta\sin\theta & 0 & b\cos^2\theta & 0 & 0 & 0 & b\cos\theta\sin\theta & 0 & -b\cos^2\theta & 0 & 0 & 0 \\
0 & 0 & 0 & 0 & 0 & 0 & 0 & 0 & 0 & 0 & 0 & 0 \\
0 & 0 & 0 & 0 & 0 & 0 & 0 & 0 & 0 & 0 & 0 & 0 \\
0 & 0 & 0 & 0 & 0 & 0 & 0 & 0 & 0 & 0 & 0 & 0 \\
-b\sin^2\theta & 0 & b\cos\theta\sin\theta & 0 & 0 & 0 & b\sin^2\theta & 0 & -b\cos\theta\sin\theta & 0 & 0 & 0 \\
0 & 0 & 0 & 0 & 0 & 0 & 0 & 0 & 0 & 0 & 0 & 0 \\
b\cos\theta\sin\theta & 0 & -b\cos^2\theta & 0 & 0 & 0 & -b\cos\theta\sin\theta & 0 & b\cos^2\theta & 0 & 0 & 0 \\
0 & 0 & 0 & 0 & 0 & 0 & 0 & 0 & 0 & 0 & 0 & 0 \\
0 & 0 & 0 & 0 & 0 & 0 & 0 & 0 & 0 & 0 & 0 & 0 \\
0 & 0 & 0 & 0 & 0 & 0 & 0 & 0 & 0 & 0 & 0 & 0
\end{pmatrix}
\tag{20}
$$

$\mathbf{C}_L^E$ defined in (19) does not include the hydrostatic corrective terms, which thus need to be added.

The derivation of $\mathbf{C}_L^E$ and $\mathbf{B}_L^E$ using transformation matrices as shown depends on the following conditions being fulfilled:

- The body-fixed coordinate system of the piston and the body-fixed coordinate system of the tube/cylinder coincide with each other.

- The equation of motion is solved by WAMIT in the body-fixed coordinate systems (Lee, 1995).

For subsequent analysis, it is necessary to know the values of the relative motion of the piston along the tube axis. In the vertical case this is straightforward, as the tube axis coincides with the heave direction. In the inclined configuration however, the response amplitude operator output by WAMIT do not directly yield values of this parameter. Again, a transformation matrix needs to be used.

$$\boldsymbol{\xi}_I = \mathbf{T}_{I/L} \cdot \boldsymbol{\xi}_L = \mathbf{T}_{I/L}^T \cdot \boldsymbol{\xi}_L \tag{21}$$

where $\boldsymbol{\xi}_I$ and $\boldsymbol{\xi}_L$ are the expressions of the response amplitude operator vector in the coordinate systems $\boldsymbol{I}$ and $\boldsymbol{L}$ respectively. The displacement along the tube axis corresponds to the displacement along the x_3-axis of the coordinate system $\boldsymbol{I}$.

6   Modelling verification

The geometry input to WAMIT is shown on figure 4. As mentioned in section 2 this geometry is a simplification of the actual device shape. The piston forms one of the bodies while the second body consists of the tube surrounding the piston and the circular cylinder breaking the free surface. Although the top cylinder and the tube are represented as disjointed parts, they are actually rigidly connected to form a single body. The presence of the surface piercing
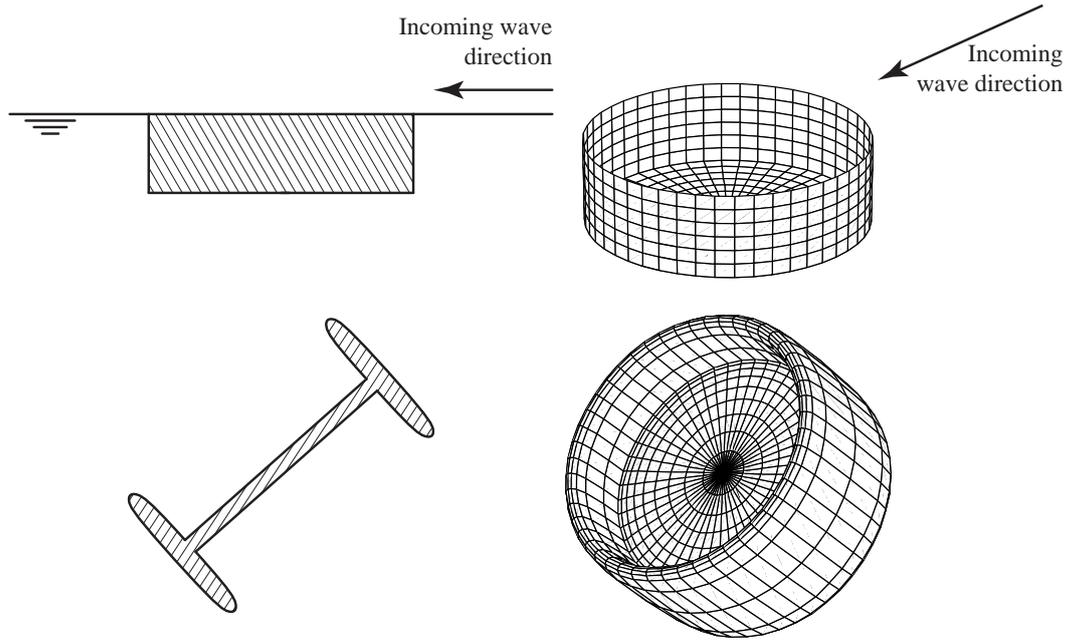
18

Fig. 4. Geometry representations of the inclined axis power take-off with a section view on the left and a 3D wireframe view on the right.

cylinder is not strictly necessary to analyse the piston's motion relative to the tube. Since both piston and tube are however fully submerged, if it were not for the top cylinder the whole system would not be subjected to any hydrostatic stiffness in heave. This would imply no resonant behaviour in heave, whereas this is a key feature of the device.

The cylinder is 0.5m in diameter. The tube axis is inclined downwave by 45° with respect to vertical. The water depth is considered infinite. The actual values for the stiffnesses are $s_t = 100\,000N.m^{-1}$ and $s_r = 100\,000N.rad^{-1}$. The density of both bodies is the same as that of water so that they are neutrally buoyant.

For symmetry reasons, only surge, heave and pitch are analysed (see section 3.2).

The WAMIT computations presented in the following paragraphs have been subjected to convergence tests aimed at finding a suitable compromise between accuracy and computation time. These tests are available in the appendix of (Payne, 2006). Modelling the hydrodynamics of bodies with thin walls can be an issue with boundary-element methods (see chapter 4 of (Faltinsen, 1990)). The piston and the tube are however thick enough to avoid this problem.

Figure 5 shows the relative excursion of the piston along the tube axis for four different damping values applied to this motion. The term 'relative' means that excursions plotted are relative to the moving tube and are not with respect to a fixed 'absolute' frame of reference. The excursions shown are normalised by wave amplitude. The relative response of the piston in the direction orthogonal to the tube axis is not shown here but its normalised values are of the order of 10^{-3} across the period range. From these results, it can be concluded that:

- The amplitude of motion diminishes consistently as the damping increases.
- The amplitude of the response in the direction orthogonal to the tube axis is negligible compared with that along the tube axis.

This confirms that the use of a transformation matrix is appropriate to derive the piston motion along the tube axis.

Another way to verify the modelling formulation relies on benchmark results obtained from WAMIT, but with the simpler single-body approach. For the two-body approach, when the relative piston motion is totally undamped, the tube/cylinder can be considered equivalent to a single body whose geometry consists of the cylinder and the tube but without any piston (see figure 6). Similarly, when the relative piston motion is heavily damped, comparison can be made with a single body where the piston is integral to the tube. This
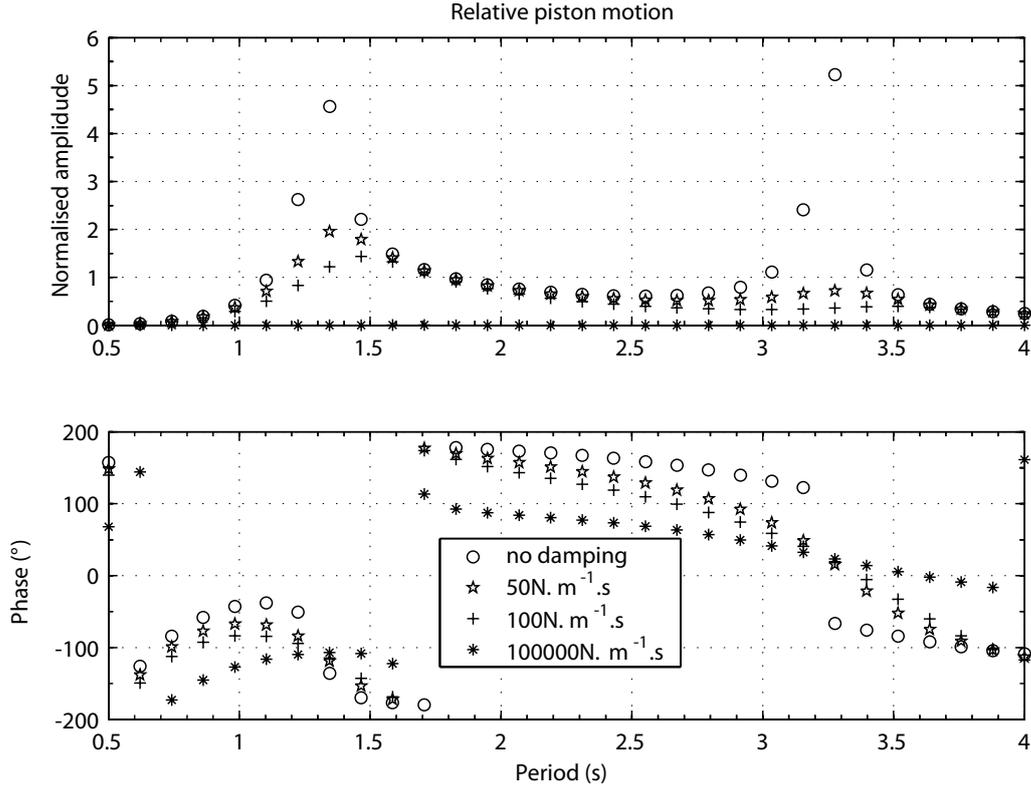
20

Fig. 5. Relative response of the piston along the tube axis for different damping values. Piston excursions are normalised by wave amplitude.

actually corresponds to the same global geometry as for the two-body approach (see figure 4) except that it is considered as only one single rigid body.

Figures 7 and 8 show the 'undamped' and 'heavily damped' comparison respectively. In both cases, the agreement is very good but with slight discrepancies in surge and pitch for the comparison between the undamped-piston and no-piston configurations. To explain these, it is useful to recall that the assumption behind this comparison is that a hollow tube is equivalent to a tube with a piston inside, free to move along the tube axis. This assumption is
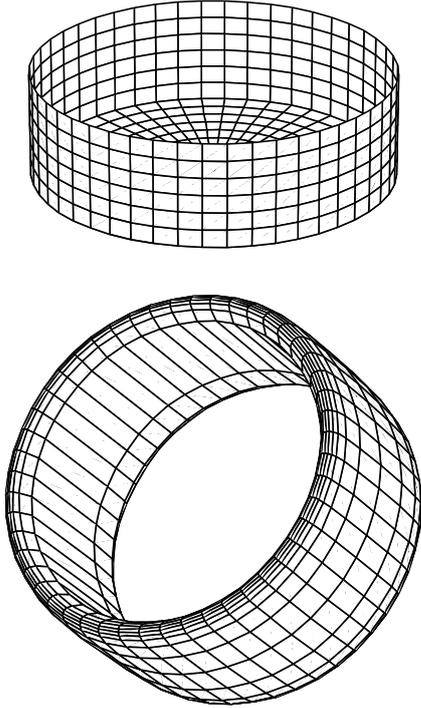
Fig. 6. Geometry of the single body approach without piston.

reasonable if, in the configuration without piston, the flow is uniform through the section where the missing piston would be. Indeed, one effect of the undamped piston is to average out the velocity profile across the whole piston surface. If in the absence of piston this profile is not uniform, the assumption of equivalence no longer applies. This is almost certainly the case in the present comparison. Also, the fact that these discrepancies are more pronounced for surge and pitch can be explained by the fact that these modes have asymmetric components with respect to the velocity profile over the piston location.

The comparisons shown in figures 7 and 8 provide reassurance that the method used to constrain and damp the piston motion is appropriate, but they also ensure that the procedure used to derive the hydrostatic coefficients is valid. Indeed, in the single-body approach, because the geometry of the body is
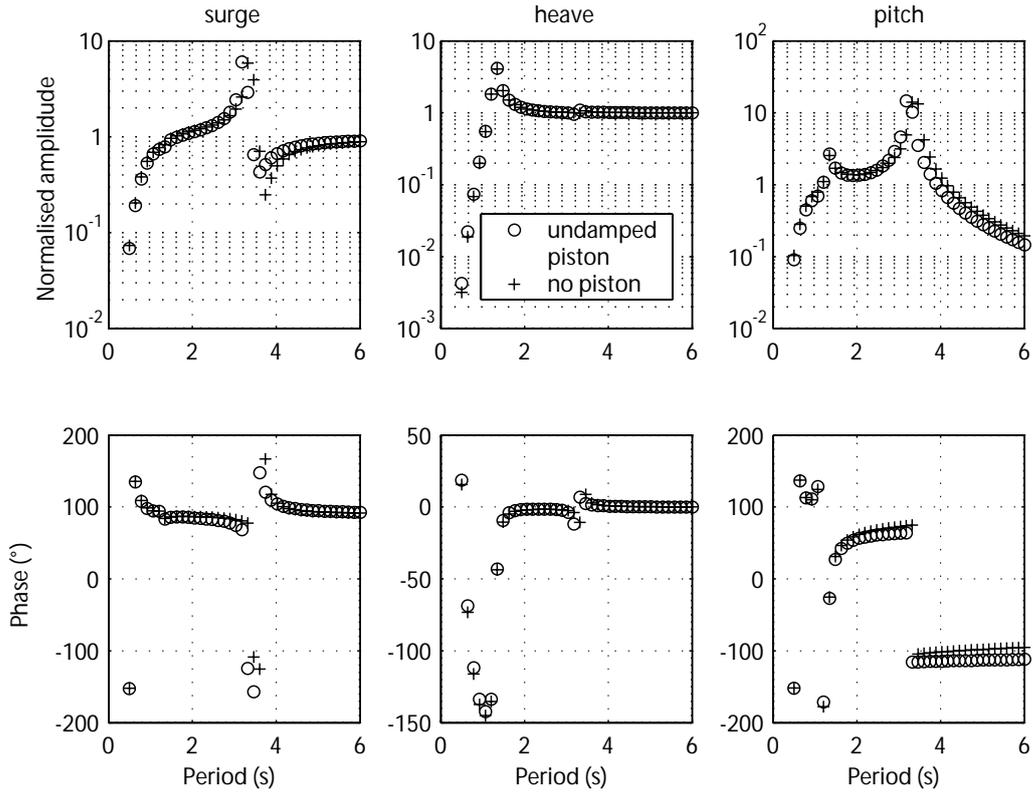
Fig. 7. Response comparisons between undamped piston and no piston configurations. Note that the y-axis scale for normalised amplitude is logarithmic.

represented by closed surfaces, the computation of the hydrostatic coefficients is directly obtained from WAMIT.

7 Conclusions

A power take-off mechanism consisting of an immersed tube with a piston sliding inside has been modelled using the boundary-element method package WAMIT. The piston and the tube have been defined as separate 'open surface' bodies. This approach required special attention in the derivation of the hydrostatic properties of the bodies. The constrain of the piston motion with
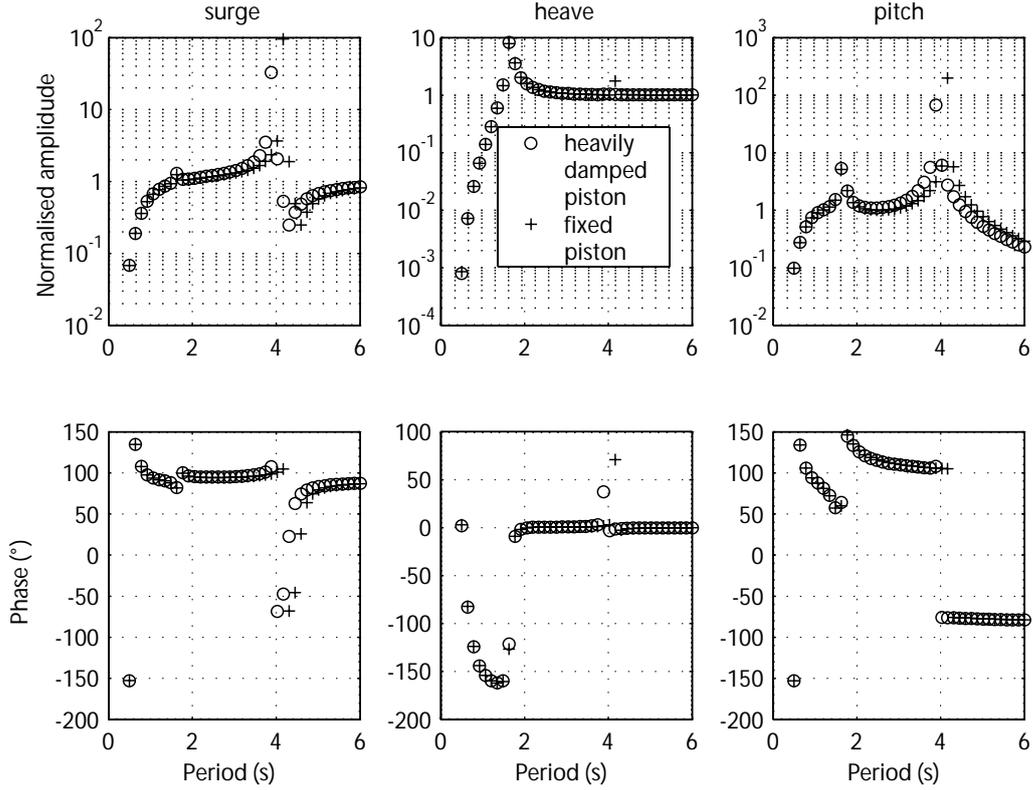
Fig. 8. Response comparison between heavily damped piston and 'fixed piston' configuration. Note that the y-axis scale for normalised amplitude is logarithmic.

respect to the tube has been achieve by introducing stiffness coefficients in the external stiffness matrix.

The modelling formulation was first derived for the case where the axis of the tube is vertical. The formulation for the sloped configuration was then obtained using transformation matrices.

The modelling has been successfully verified by comparison against bench mark computations obtained from WAMIT for single body approaches. Validation against experimental measurement will be investigated in a subsequent paper.

24

References

Bergdahl, L., October 1992. Review of research in Sweden. In: Wave energy R&D workshop. Commission of the European Communities, Cork, Ireland, pp. 129–136.

Delauré, Y., Lewis, A., 2003. 3D hydrodynamic modelling of fixed oscillating water column wave power plant by a boundary element methods. Ocean Engineering, 309–330.

Eatock Taylor, R., Jefferys, E., 1986. Variability of hydrodynamic load predicitions for a tension leg platform. Ocean Engineering 13 (5), 449–490.

Faltinsen, O., 1990. Sea loads on ships and offshore structures. Cambridge University Press.

Herfjord, K., Nielsen, F., 1992. A comparative study on computed motion response for floating production platforms: Discussion of practical procedures. In: Conference on the Behaviour of Offshore Structures (BOSS '92). London.

Lee, C.-H., 1995. WAMIT theory manual. Massachusetts Institute of Technology, available from www.wamit.com.

Lee, C.-H., Newman, J., Nielsen, F., May 1996. Wave Interactions with an Oscillating Water Column. In: 6th International Offshore and Polar Engineering Conference. Vol. 1. Los Angeles, USA, pp. 82–90.

Mortenson, M., 1997. Geometric Modeling, 2nd Edition. John Wiley & Sons.

Newman, J., 1977. Marine Hydrodynamics. The MIT Press.

Payne, G., 2006. Numerical modelling of a sloped wave energy device. Ph.D. thesis, The University of Edinburgh.

Salter, S., Lin, C.-P., November 1995. The sloped IPS wave energy converter. In: 2nd European Wave Energy Conference. Lisbon, Portugal, pp. 337–344.

WAMIT, Inc., 2000. WAMIT user manual Version 6.0, 6.0PC, 5.3S. Available from www.wamit.com.